ELSEVIER

Journal of Structural Geology 29 (2007) 881–897

JOURNAL OF STRUCTURAL GEOLOGY

www.elsevier.com/locate/jsg

Deformation sequence of Baltimore gneiss domes, USA, assessed from porphyroblast Foliation Intersection Axes

Meng-Wan Yeh*

Department of Earth Sciences, National Taiwan Normal University, No. 88 Ting-Chou RD 4th Division, Taipei 117, Taiwan

Received 18 January 2006; received in revised form 6 December 2006; accepted 14 December 2006
Available online 27 December 2006

Abstract

The NE-SW trending gneiss domes around Baltimore, Maryland, USA, have been cited as classic examples of mantled gneiss domes formed by diapiric rise of migmatitic gneisses [Eskola, P., 1949. The problem of mantled gneiss domes. Quarterly Journal of Geological Society of London 104/416, 461–476]. However, 3-D analysis of porphyroblast-matrix foliation relations and porphyroblast inclusion trail geometries suggests that they are the result of interference between multiple refolding of an early-formed nappe. A succession of six FIA (Foliation Intersection Axes) sets, based upon relative timing of inclusion texture in garnet and staurolite porphyroblasts, revealed 6 superposed deformation phases. The successions of inclusion trail asymmetries, formed around these FIAs, document the geometry of deformation associated with folding and fabric development during discrete episodes of bulk shortening. Exclusive top to NW shear asymmetries of curvature were recorded by inclusion trails associated with the vertical collapsing event within the oldest FIA set (NE-SW trend). This strongly indicates a large NE-SW-striking, NW-verging nappe had formed early during this deformation sequence. This nappe was later folded into NE-SW-trending up-right folds by coaxial shortening indicated by an almost equal proportion of both inclusion trail asymmetries documented by the second N-S-trending FIA set. These folds were then amplified by later deformation, as the following FIA sets showed an almost equal proportion of both inclusion trail asymmetries.

Keywords: Nappe; Porphyroblasts; Foliation Intersection Axes; Gneiss domes

1. Introduction

Gneiss domes are a common feature of many orogenic belts that tend to be aligned with the trend (e.g., Eskola, 1949; Duckan, 1984; Andersen et al., 1998; Dorais et al., 2001; Teyssier and Whitney, 2002). Yet the origin of gneiss domes was interpreted in differing models, including diaprism (Eskola, 1949; Teyssier and Whitney, 2002), fold interference (Hopson, 1964; Fisher et al., 1979; Duckan, 1984; Kodama and Chapin, 1984; Muller and Chapin, 1984; Aerden, 1994, 1998; Bell et al., 2005), extension-controlled exhumation (Viruete, 1998; Lee et al., 2004) and duplex-related folding (Burg et al., 1984). With metamorphic isograds, foliation and layering of the gneiss lying parallel to the circular to elliptical map patterns, Eskola (1949) suggested that the gneiss domes around Baltimore, Maryland, USA, were mantled diapiric gneiss domes. Bromery's (1968) aeromagnetic and gravity work showed the expected gravity low associated with the Towson and Chattolanee domes but not for the Phoenix dome (Fig. 1), casting doubts on Eskola's model. Further gravity and petrology studies (e.g., Hopson, 1964; Wetherill et al., 1966; Fisher et al., 1979; Kodama and Chapin, 1984; Muller and Chapin, 1984; Olsen, 1999) suggested an alternative model that these domes are interference structures formed by refolding of an early recumbent nappe. However, Teyssier and Whitney (2002) argued that with positive feedback between decompression and near-isothermal melting at mid-crustal levels, many diapiric gneiss domes could be formed.

Regional-scale folds of compositional layering commonly preserve evidence for long and complex deformation histories on microscopic and mesoscopic scales (e.g., Smith and Marshall, 1992; Ratcliffe et al., 1992; Adshead-Bell and

* Tel.: +886 2 2934 7120x41; fax: +886 2 2933 3315.
E-mail address: marywyeh@msn.com

0191-8141/$ - see front matter © 2007 Elsevier Ltd. All rights reserved.
doi:10.1016/j.jsg.2006.12.003

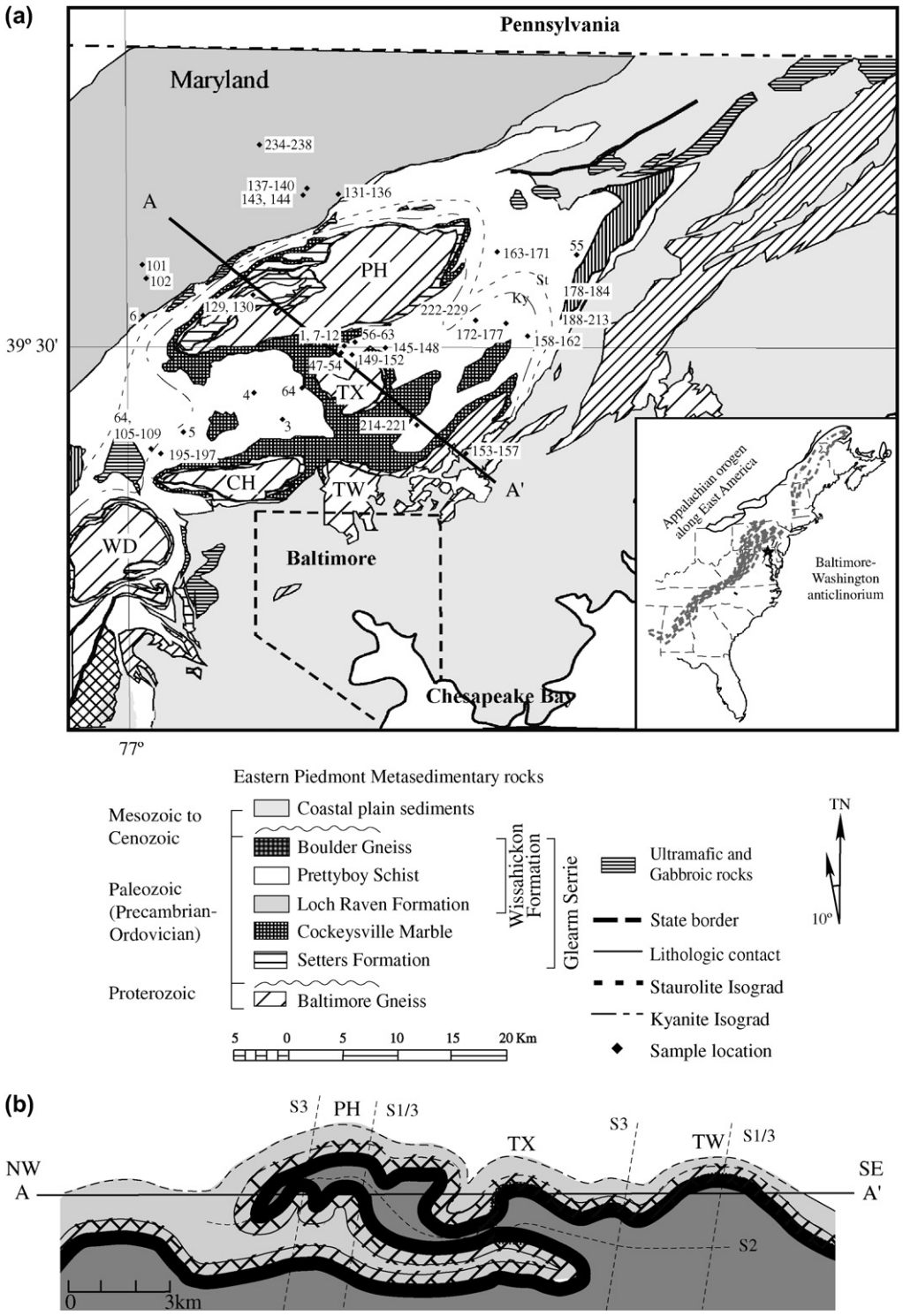

Fig. 1. (a) Detailed geological map; and (b) schematic cross section through line A-A′ of the Baltimore area, Maryland, modified from Cleaves et al. (1986) and Muller and Chapin (1984). PH is Phoenix, TX is Texas, TW is Towson, CH is Chattoanee, WD is Woodstock, MF is Mayfield, and CL is Clarksville. The dashed line defines an interpreted lithological contact above ground. The dotted lines define the axial planes (S_2 and S_3) of different fold generations.

Bell, 1999). Understanding the spatial and temporal development of such macroscopic folds within multiple-deformed terrains provides important constraints on tectonic models of continental collision. Correctly correlating such folds to portray an overall deformation history can be difficult due to their size. Commonly, timing has been determined based on the principle that minor folds and crenulation cleavages switch vergence (or crenulation asymmetry) from one limb to the other of a macroscopic fold of the same age (e.g. Hobbs et al., 1976). However, complications can arise where a superficially simple fold geometry was formed via a polyphase deformation history, during which the initial fold shape was

repeatedly modified but not destroyed. Recognition of such polyphase histories is usually complicated by repeated reactivation of an early-formed schistosity during the subsequent deformation phases, while development of new (superposed) crenulation cleavages remain restricted to zones of relatively low-strain. Here, they can be potentially preserved by porphyroblasts growing in these zone (Williams, 1985; Bell, 1986; Johnson, 1992; Davis and Forde, 1994; Ham and Bell, 2004; Bell et al., 2005).

Bell and Johnson (1992), Hickey and Bell (2001) and Bell et al. (2003) showed that the differentiation asymmetry of a crenulation cleavage, that is the sense in which the crenulated fabric curves from quartz-rich microlithons into mica-rich cleavage septae, does not necessarily switch across macroscopic folds, despite apparently forming the axial-plane fabric of that fold. This can be due to: (1) a two-stage folding process, in which a fold was formed by shearing the pre-formed vertical differentiated cleavage (stage one) into flat foliation (stage two; e.g. Fig. 3 in Bell et al., 2003). The foliation asymmetries remain the same across the fold if the shear sense remain unchanged from stage one to stage two. (2) A succession of alternate deformations can form crenulation cleavage with similar orientation to the axial plane foliations after the macroscopic fold. Foliation-foliation asymmetry may identify a fold, but it does not necessarily time a fold if a later fold developed directly over the top of an earlier one with the same axial plane orientation.

During the past two decades, complex inclusion trail geometries have been increasingly re-interpreted in terms of successively included crenulation cleavages (e.g. Bell and Johnson, 1989; Bell and Hayward, 1991; Bell et al., 1998; Aerden, 1998, 2004) rather than progressive porphyroblast rotation (Powell and Vernon, 1979; Rosenfeld et al., 1988). Axes of inclusion trail curvature have been, consequently, re-interpreted as fossilized crenulation axes or intersection lineation between two foliations preserved in the porphyroblast. Multiple thin-sectioning techniques have been developed to accurately measure the orientation of inclusion trail curvature axes now known as "FIA" (Foliation Intersection or Inflexion Axes). Such FIAs have been found to exhibit regionally consistent orientations in many orogens (e.g., Hickey and Bell, 2001; Bell et al., 2004; Yeh and Bell, 2004) where they can commonly be classified into a discrete number of age sets with distinctive geographical trends and consistent relative timings. The relative timing is given by key-porphyroblasts that contain two or more FIAs in progressive (core-median-rim) growth zones. The present work documents six FIA sets in the Baltimore Gneiss Dome region, as well as the asymmetry of inclusion trail curvature associated with each of these sets, in order to study the timing and formation mechanism of the Baltimore gneiss dome.

2. Geological setting

Anticlines within the Baltimore Gneiss in the vicinity of Baltimore City, Northeast Maryland, USA, include the Phoenix, Texas, Chattolanee and Towson domes that lie along the culmination of the doubly-plunging Baltimore-Washington anticlinorium (Fig. 1a; Fisher, 1970). The Grenville-age (1200–1000 Ma) Baltimore Gneiss is composed of layered quartzo-felspathic, migmatite inter-layered with hornblende gneiss and amphibolite (Hopson, 1964; Crowley et al., 1975; Crowley and Reinhardt, 1975, 1980; Crowley et al., 1976a,b), and forms the core of these domal anticlines. These Mesoproterozoic rocks (Aleinikoff et al., 1997) were interpreted as part of the Laurentian continental basement or as remains of a Baltimore microcontinent (Drake, 1989; Drake et al., 1989; Pavlides, 1989). Late Precambrian to Early Paleozoic metasedimentary rocks of the Glenarm series unconformably overlie the Baltimore gneiss (Fisher, 1970). The Glenarm series contains three formations: Setters Formation, Cockeysville marble and the Wissahickon Formation (Fisher, 1970; Fig. 1a). The age and stratigraphic successions within the Glenarm series have been extensively studied over the past 80 years, and the stratigraphic nomenclature has been revised frequently (e.g., Southwick and Fisher, 1967; Higgins and Fisher, 1971; Higgins, 1972; Crowley, 1976; Seiders and Higgins, 1976; Williams, 1978). This paper follows the stratigraphic nomenclature and sequence proposed by Fisher (1970), Moller (1979) and Muller (1991) because these units can be applied to all the locations described in this paper.

2.1. Deformation

Geological mapping, structural analysis, and gravity and magnetic modeling indicate that the Phoenix, Texas, Chattolanee, and Towson gneiss anticlines are part of a large refolded crystalline nappe system rooted beneath the Towson domes (Kodama and Chapin, 1984; Muller and Chapin, 1984; Fig. 1b). Three deformation stages had affected the pelitic schists around the Baltimore Gneiss terrane (Hall, 1988; Table 1). Continued thrusting during the Ordovician Taconic Orogeny (Sinha and Hanan, 1987) caused the collision of the Baltimore mafic complex island arc terrane with the Baltimore Gneiss terrane, attributed to nappe formation (Kodama and Chapin, 1984; Muller and Chapin, 1984). Although radiometric ages indicate that the Grenville metamorphism had affected the Baltimore gneiss (Tilton et al., 1970; Muller and Chapin, 1984), no structural evidence for Grenvillian tectonic history was found since the structural elements that accompanied this tectonism were obliterated or completely obscured by subsequent Appalachian tectonism (Muller and Chapin, 1984). The doubly-plunging NE-SW-trending Baltimore Gneiss anticlines form the major visible map-scale structures (Fig. 1b; Cloos, 1964; Crowley et al., 1976a,b; Crowley, 1977; Moller, 1979; Muller and Edwards, 1985; Muller, 1991). These refolded tight to isoclinal folds (F_2, Table 1) produced the dominant upright schistosity, and are well documented throughout the Maryland Piedmont (Freedman et al., 1964; Fisher, 1970; Higgins, 1973; Muller and Chapin, 1984). Subsequent vertical shortening has formed open to isoclinal F_3 folds in S_2 with sub-horizontal axial planes and cleavages that crenulated earlier foliations; Table 1).

Table 1
Correlation of structures of the Baltimore gneiss anticlines

Proposed deformation ages	Freedman et al. (1964)	Cloos (1964)	Wise (1970)	Fisher (1970)	Muller and Chapin (1984)	This study
Alleghanian (260–190 ma.)						
	F_3	F_1/F_2	F_3	F_4	$F_{3/\text{brittle faulting}}$ F_{2c}	Matrix D_4 Matrix D_3
Taconic – Acadian (360–500 ma.)						
	F_2		F_2	F_3	F_{2b}	Matrix D_2 & D_1 Refolding of nappe
	F_1		F_1	F_2 F_1	F_{2a}	Nappe development
Grenville (1000–1200 ma.)					F_1	

2.2. Metamorphism

Metamorphism accompanying deformation during orogenesis extended from the Taconic (510 to 460 Ma) to the early Acadian (408 to 360 Ma; Tilton et al., 1970; Fisher, 1971; Grauert, 1973a,b; Lang, 1990; Sinha et al., 1997; Aleinikoff et al., 2002). Bosbyshell et al. (1998, 1999) indicated that the Wissahickon formation experienced two main stages of Paleozoic metamorphism. An earlier andalusite-sillimanite facies (4–6 kbars; ~480 Ma) was variably overprinted by a kyanite-bearing Barrovian sequence (550–650 °C, 7–9 Kbars; ~380 Ma; or 625–675 °C, 7–9 Kbars; Fisher and Olsen, 2004). Lang (1996), however, pointed out that only one protracted metamorphic episode had affected the nappe formation, and interpreted that metamorphism peaked between 520 to 600 °C and 4.6 to 7.4 kilobars within the staurolite + kyanite to kyanite + sillimanite zones (Lang, 1990, 1991). Plank (1989) determined that the peak metamorphic temperatures and pressures varied from 600 ± 50 °C and 5 to 6 kbars in the west to 750 ± 50 °C and 6 to 7 kbars in the east.

The highest-grade metamorphic assemblages are observed at the contacts of the gneiss (Hall, 1988; Lang, 1990). Both temperature and pressure seem to have decreased from both limbs towards the hinge regions of synclines within the gneiss domes. Many studies (Doe et al., 1965; Southwick and Owens, 1968; Fig. 1a) noted that the general isograd pattern reflects the outline geometry of gneiss domes from the garnet zone at the rim to the kyanite zone toward the center. Plank (1989) suggested that this west to east increase in metamorphism is due to differential uplifting, and the peak metamorphism was attained prior to refolding of the gneiss-cored nappe (Fisher et al., 1979; Hall, 1988; Lang, 1990).

3. Methods

Foliation Intersection/Inflection Axes (FIA; Fig. 2a) were measured and correlated from orientated samples using the techniques of Hayward (1990). For each oriented rock sample, six vertical thin sections were cut in 30° increments around the compass to determine the geometry of the structures in 3D (Fig. 2b). Inclusion trails within porphyroblasts were examined in each thin section together with matrix foliations. At least 10 porphyroblasts of one mineral type were examined for each thin section. FIA are determined by recording the asymmetry switch of equivalent inclusion trail curvatures when viewed from the same direction in a series of differently striking vertical thin sections of an oriented samples that fan about the compass (Fig. 2b,c). Extra thin sections at 10° intervals were cut between the sections where the inclusion trail asymmetry (clockwise or anticlockwise) of curvature switched. The FIAs was determined as lying between the 10° sections where the asymmetry flips (Fig. 2; e.g. Hayward, 1990; Bell et al., 1995, 1998). FIAs were measured from oriented rock samples relative to both geographical coordinates and the normal to the earth surface.

Systematic correlation between inclusion trail curvatures within a specimen for determining the FIA orientations, and correlating FIAs between specimens to distinguish temporally-related sets, are the two major components of this study. Statistical tests such as the Watson's U^2 test modified for grouped axial data (Upton and Fingleton, 1989; Yeh, 2003; Yeh and Bell, 2004) and X^2 test (Bell et al., 1998; Yeh, 2003; Yeh and Bell, 2004), have been applied to determine whether the multi-modal nature is significant. The succession of differently trending FIAs preserved from core to median to rim in multi-FIA samples provides a way to distinguish different FIA sets and establishes their relative timing. The changes in orientation between core and rim FIA populations appear to be due to a timing difference for the formation of foliations trapped as inclusion trails within the porphyroblasts (Bell et al., 1998; Yeh and Bell, 2004).

4. Mineral assemblages and textures

All samples contain quartz, plagioclase, muscovite, biotite, garnet and opaque minerals such as ilmenite and magnetite. Retrograde chlorite is also observed in some samples, though Lang (1996) indicated the presence of prograde chlorite. Five different mineral assemblages of biotite-garnet-staurolite; biotite-garnet-staurolite-kyanite; biotite-garnet-kyanite; biotite-garnet-staurolite-kyanite-sillimanite and biotite-garnet-kyanite-sillimanite have been observed within the regional kyanite isograd. No systematic differences were observed between assemblages in pelitic schists throughout the Baltimore

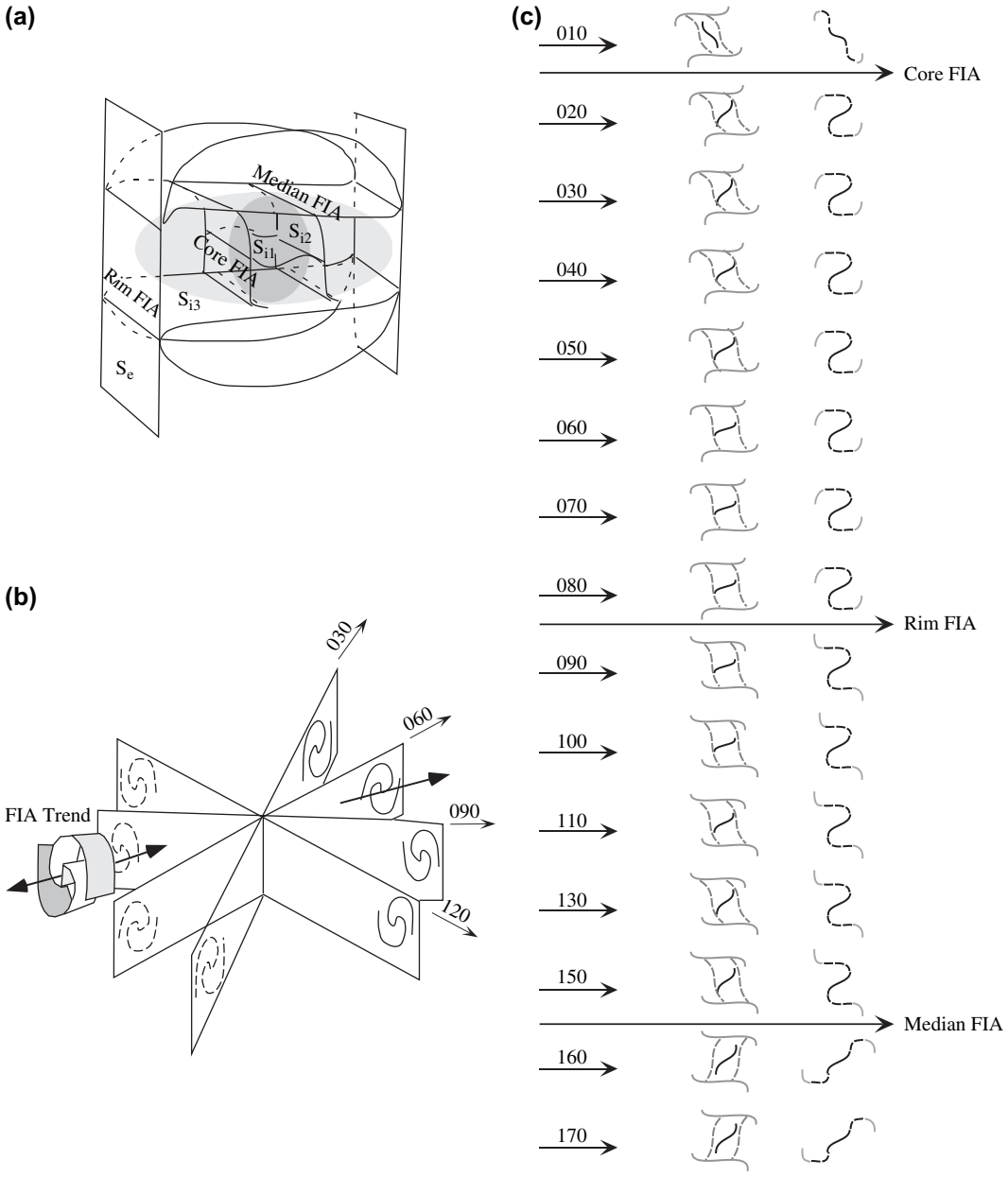

Fig. 2. Schematic diagrams showing the location of FIA relative to foliations within a porphyroblast with multiple growth episodes (modified from Bell et al., 1998). (a) 3-D cross section sketch of an euhedral porphyroblast with 3 internal foliations (S_{i1}, S_{i2} and S_{i3}) and one matrix foliation (Se). The intersection lineations between these foliations are FIAs. (b) 3-D sketches showing the method of using oriented thin sections to determine the FIA orientation. The asymmetry of inclusion trail curvature switches when viewed in the same direction on thin sections across a FIA. (c) Sketches of inclusion trail patterns correlation to (a) from vertical thin sections with various strikes. 3 FIAs of 15° (core), 155° (median) and 85° (rim) with temporal correlation can be distinguished. Black solid line indicates the core inclusion trail, black dashed line for the median inclusion trail, and gray line for the rim inclusion trail.

region. Lang (1990, 1991) interpreted that the temperature and total pressure are nearly constant between 520 to 600 °C and 4.6 to 7.4 kilobars. She suggested the non-systematic distribution of these mineral assemblages within the kyanite isograd should reflect the variations in bulk composition and/or metamorphic fluid composition.

4.1. Mesostructures preserved in the matrix

Four matrix fabrics (S_1, S_2, S_3 and S_4; Figs. 2 and 3), associated with successive deformation described events (Table 1), were correlated from sample to sample and outcrop to outcrop using consistency in the orientation and the overprinting succession of folds, foliations and crenulations. The oldest schistosity S_1, mostly observed under the microscope, is preserved as crenulations between the seams of differentiated cleavage S_2 (Fig. 3). S_2 is generally the earliest deformational fabric preserved in the matrix that is also macroscopic in the field. S_2 is axial planar to the macroscopic 10°–30°-trending folds (F_2) of compositional layers (Fig. 3a). S_2 is a spaced differentiated crenellation cleavage in thin section (Fig. 3a) that is generally parallel to compositional layers, suggesting strong

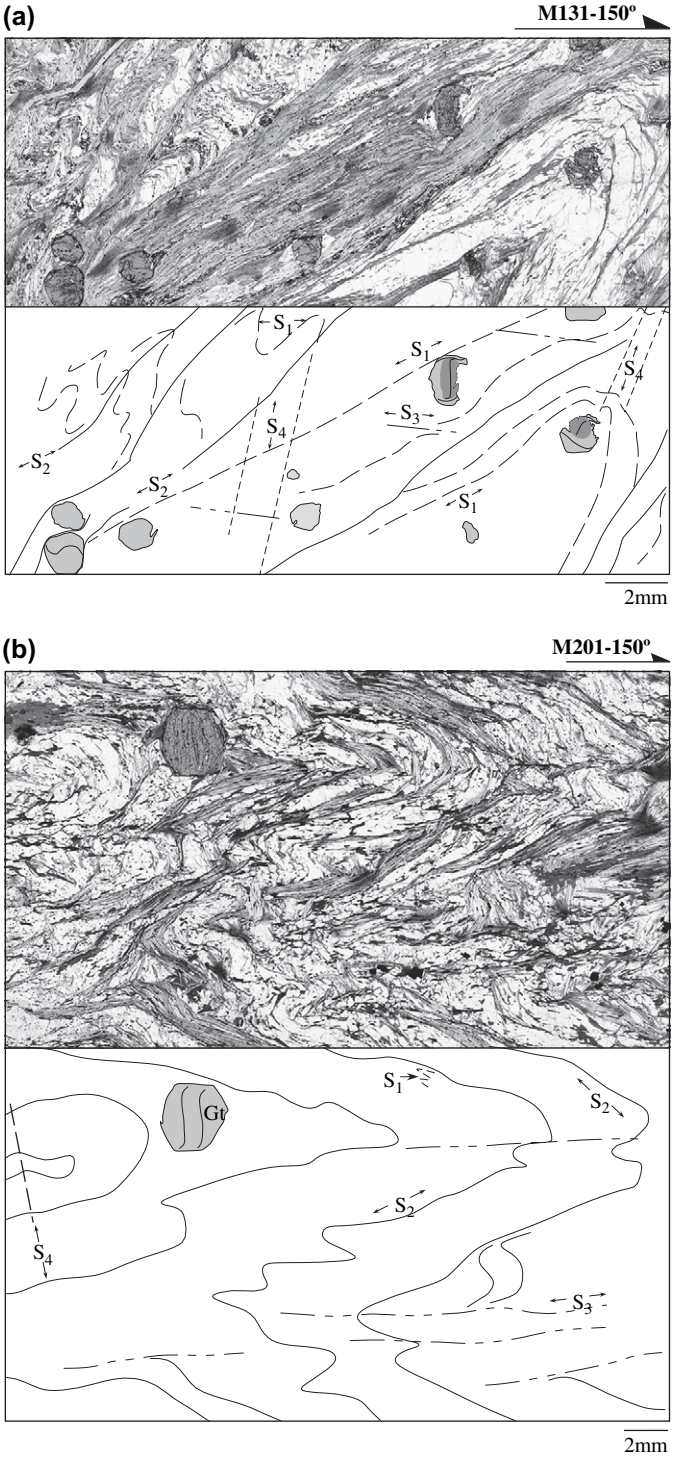

Fig. 3. Microphotograph and accompanying line diagram illustrating the sequence of matrix foliation from S_1 to S_4. Vertical thin section, arrow indicates strike, plane polarized light. (a) S_1 is folded with an originally steeply-dipping axial plane, S_2. Weak crenulations form a local subhorizontal S_3 that sheared the steep S_1 and S_2. Subvertical differentiated crenulations, S_4, reactivated and steepened the dominant S_2 matrix foliation. Garnet porphyroblasts contain distinguishable cores and rims with inclusion trails truncated by S_1 and S_2 foliations. (b) S_1 is only preserved locally and was folded with axial plane S_2. S_2 is the dominant foliation observed that is folded with sub-horizontal axial plane S_3. Both S_2 and S_3 are gently folded about steep axial planes S_4. Garnet porphyroblast contains curved inclusion trails truncated by S_2.

reactivation of bedding during folding (e.g., Bell, 1986). S_3 is generally sub-horizontal axial planer to F_3 folds (Fig. 3b). D_4 produced a weak crenulation with steeply NW-dipping axial planes (S_4) that are locally observed (Fig. 3) where S_2 and S_3 are weakly crenulated.

5. Microstructures preserved in the porphyroblasts

5.1. Garnet

A total of 143 FIAs were determined and measured from garnet porphyroblasts in 87 oriented specimens. 47 specimens contain multiple FIA measurements allowing temporal relationship determination (Table 2; Fig. 4a). Statistic results for garnet FIAs (Table 3) greatly exceeds the upper 5% critical value (Yeh, 2003; Yeh and Bell, 2004), suggesting the polymodal FIA trends observed in Fig. 4a are statistically meaningful and can be separated into groups. However, the fluctuations seen from rose diagrams (Fig. 4a) do not allow clear interpretation of meaningful peaks or modes. The FIA data, with 10 degree class intervals, were smoothed by applying a moving average with order $N = 5$ (pie segment = 50° interval) to discernment different modes (Fig. 4c; King, 1994; Yeh, 2003; Yeh and Bell, 2004). 6 sets of FIA populations with general peaks of $47° \pm 13°$, $0° \pm 7°$, $89° \pm 12°$, $143° \pm 8°$, $8° \pm 22°$ and $83° \pm 5°$ can be distinguished (Fig. 4a,c).

5.2. Staurolite

A total of 34 FIAs were determined and measured from staurolite porphyroblasts in 26 oriented specimens (Fig. 4b). 16 FIAs were measured from 8 specimens that each contain both core and rim FIAs (Table 2). Most inclusion trails are sigmoidal or straight in geometry that are either continuous with or truncated by the dominant matrix foliation S_2 (Fig. 5a). Similar to FIAs in garnet, FIAs in staurolite are statistically non-random (Yeh, 2003; Yeh and Bell, 2004; Table 3). 5 general groups of FIA sets A to E, with trends peaking at: $172° \pm 7°$, $103° \pm 15°$, $132° \pm 10°$, $173° \pm 9°$ and $81° \pm 24°$, can be separated according to the peaks and troughs suggested by moving averages and rose diagrams (Fig. 4b,c).

6. Relative timing of porphyroblast growth and their FIA succession

Textural relations of inclusion trails between porphyroblasts and matrix foliations (Hall, 1988; Vernon, 1988; Bell et al., 2003) allow a relative timing of growth to be elucidated. Most inclusion trails in garnet porphyroblasts formed before the S_1 as they are truncated by the matrix foliations (Figs. 3 and 5). The inclusion trails are composed mostly of elongate grains of quartz, mica and ilmenite that are much finer than the coarse-grained matrix (Figs. 3 and 5). Two generations of garnet porphyroblast growth can be distinguished from core-rim relations. Some specimens have garnet containing inclusion-free core, while other specimens show sigmoidal trails in the core

Table 2
Time succession of FIA peaks indicated by multi-FIA samples measured from garnet (Gt) and staurolite (St) porphyroblasts

		Time (old >>>>>>>> to >>>> > > > > young)					
Statistical peaks:	Gt	Set I (47° ± 13°)	Set II (0° ± 7°)	Set III (89° ± 12°)	Set IV (143° ± 8°)	Set V (8° ± 22°)	Set VI (83° ± 5°)
	St		Set A (172° ± 7°)	Set B (103° ± 15°)	Set C (132° ± 10°)	Set D (173° ± 9°)	Set E (81° ± 24°)
M3	Gt	45	5				
M145	Gt	55	0				
M62	Gt	25	5	120			
M64	Gt	30–60		60–90			
M149	Gt	40			120–150		
M12	Gt	35				175	
M174	Gt	60				45	
M1	Gt		175	70			
M48A	Gt		10	95			
M54B	Gt		15	60			
M57	Gt		25	55			
M59	Gt		0–30	95			
M132	Gt		150–180	55			
M146	Gt		15	70			
M155	Gt		150–180	60			
M166	Gt		150–180	95			
M225	Gt		170	115			
M63	**Gt**		**175**	**125**			
	St				**130**	**170**	
M161	**Gt**		**10**				
	St			**90–120**		**5**	
M105	Gt		10–30	115	130		
M182	**Gt**			**85**			
	St		**170**		**110–150**		
M164	Gt		150–180	90–120		25	
M4	Gt		25		155		
M5A	Gt		150–180		130–150		
M5B	Gt		150–180		130–150		
M61	Gt		0–20		120–150		
M160	Gt		5		150–170		
M167	Gt		5		120–160		
M49	Gt		5		135	20	
M9A	Gt		165			175	
M50	Gt		0–30			175	
M51	Gt		165			175	
M130	Gt		20			175	
M203	Gt		5			10	
M205	Gt		5			170–190	
M206	Gt		165			10	
M158	Gt		175			0–30	80
M201	Gt		150–180			0–40	60–80
M183	Gt		177				62–92
M204	Gt			100	145		
M60	Gt			90–110			85
	St			100	120–150		
M223	**Gt**			**90–120**		**25**	
	St			**90–120**	**120–150**		
M180	Gt			125	140	175	
M178	Gt			80			85
M215	Gt			65			75
M48B	Gt				150	150–170	
M53	Gt				155	165	
M207	Gt				150	10	
M163	St				145		60–90
M176	St					2	110

truncated by inclusion trails in the rim. However, apart from sample M5A, most of the trails in the rims are discontinuous to matrix foliation, suggesting the matrix foliations formed much later than the growth of garnet porphyroblasts during a long and complex deformation history. Garnet porphyroblasts with inclusion-free rims might have grown during matrix foliation development, but no timing criteria are available to demonstrate this.

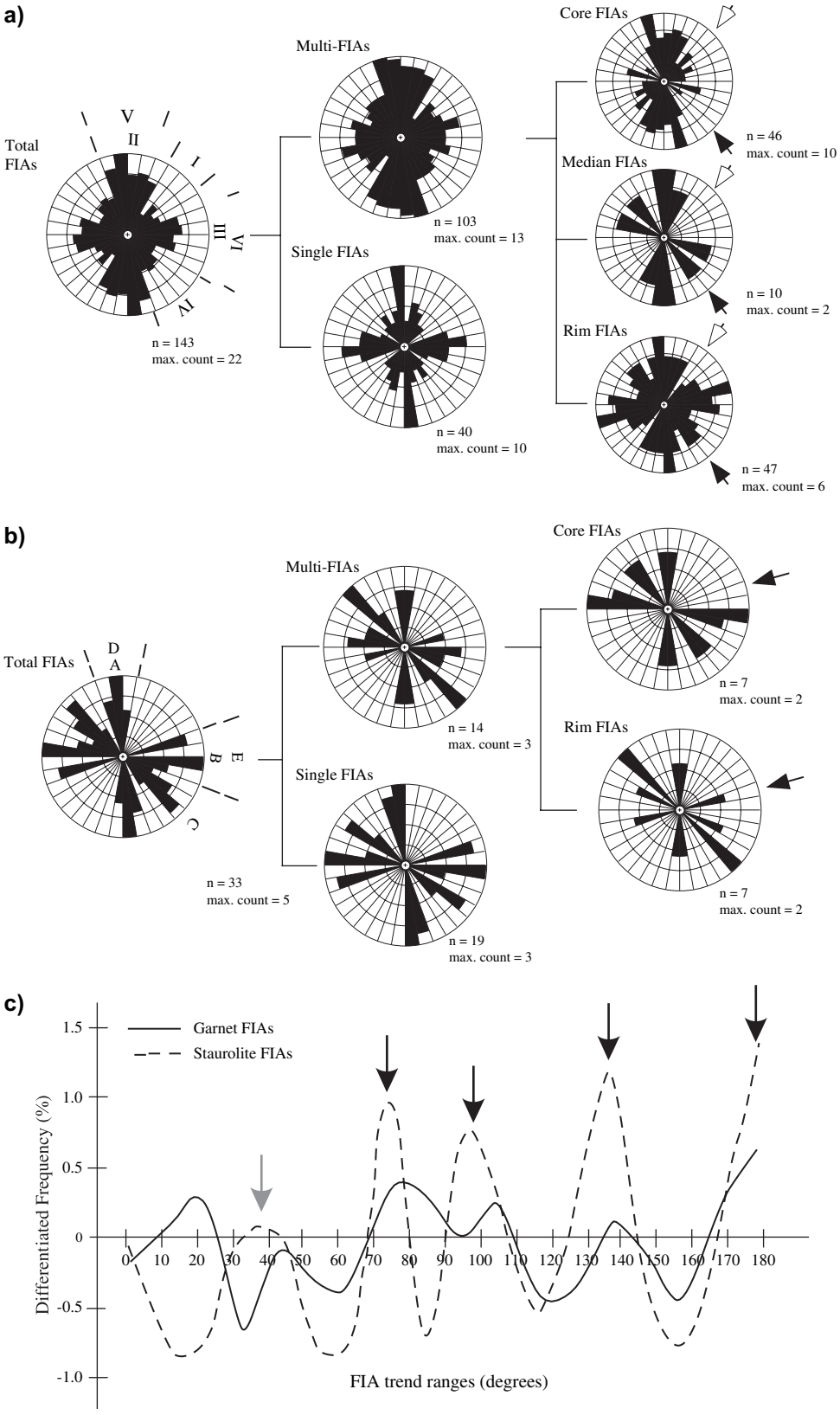

Fig. 4. FIA trends and their relative timing measured in garnet and staurolite porphyroblasts. Equal area (radii = square root of frequency) rose diagrams, with a 10° class interval, the FIA trends are grouped as total FIA trend measurements, multi-FIA population, single-FIA population, core-, median-, and rim-FIA populations within multi-FIA population. (a) FIAs measured from garnet porphyroblasts. The oldest garnet FIA set indicated by open arrow was only observed in the core FIA population, while the younger garnet FIA set IV, indicated by filled arrow, is missing from the core FIA population, but present in both median and rim FIA populations. (b) FIAs measured from staurolite porphyroblasts. (c) Smoothed frequency distributions of all garnet (solid line) and staurolite (dash line) FIAs with 10° class interval and order $N = 5$ (pie segment = 50°). Four distinct peaks between 70°−80°, 90°−110°, 130°−150° and around 170° are both observed for garnet and staurolite FIAs. Weak peaks around 40° is observed for staurolite and garnet FIAs. An additional peak around 20° is only indicated by garnet FIAs, which is missing for staurolite FIAs.

Table 3
Test of the null hypothesis, H_0, that the total, single and multi FIAs measured from garnet and staurolite porphyroblasts around the Baltimore region are samples of a random population using Watson's U^2 test statistic for grouped data

	n_i	n_{pj}	S_i	S_i^2	U_G^2
Garnet					
Total	142	2.972	−182.500	4128.171	0.624
Single	40	1.111	−122.000	810.620	0.222
Multi	102	2.822	−49.500	1872.894	0.487
Staurolite					
Total	22	0.917	−201.500	1481.208	0.297
Single	19	0.528	−146.500	19.000	0.175
Multi	14	0.289	−55.000	14.000	0.174

j = groupings defined with a 10 degrees interval from 0° to 260°. n_j = the number of FIA trends measured within each group range. n_{pj} = the expected value for each group defined by the average value over j groups. S_i = the accumulated difference between the expected value (n_{pj}) with the observed value (n_j). U_G^2 values are defined with $U_G^2 = 1/\text{nk}\ (s_i^2 - 1/k(S_i)^2)$ with critical value of 0.187 at the 0.05 level of significance. FIA trends were initially doubled to convert them from axial to directional data: modulo 260°.

Numerous specimens contain staurolite porphyroblasts that are wrapped by/or parallel to S_2 and/or S_3 (Fig. 5a) suggesting that these staurolite porphyroblasts have grown during or post D_2 (Zwart, 1960; Bell, 1986). As shown in Fig. 5a, garnet porphyroblasts also occur locally as inclusions within staurolite, which suggests garnet growth commenced earlier than other porphyroblastic phases. However, a few specimens around the Phoenix dome, within the kyanite zone, contain garnet porphyroblasts with staurolite inclusions (Fig. 5b), indicating that, locally, younger garnet growth has occurred (Hall, 1988; Lang, 1990, 1996). It is difficult to determine the relative timing between staurolite and kyanite porphyroblasts since they are usually intergrown and both contain inclusion trails continuous and/or truncated by matrix foliation (Fig. 5a,c). Examples showing staurolite, kyanite and/or fibrolitic sillimanite, as inclusions in the rims of garnet porphyroblasts, suggest garnet growth continued after staurolite and kyanite. Based on the inclusion relation described above, the order of porphyroblast growth appears to be garnet, staurolite + 2nd garnet growth, and staurolite + kyanite + 3rd garnet growth.

Similar mineral growth history was also determined by Lang (1996). By successfully modeling the complex garnet zoning with Gibbs-method, Lang (1996) indicated 3 growth episodes for garnet porphyroblasts, which began at 550 °C and 6.5 Kbars in the assemblage chlorite + biotite + garnet + muscovite + plagioclase + quartz. Staurolite was added to the assemblage when some garnet was consumed with increasing temperature and first decreasing followed by constant pressure (at 570 °C and 5.7 Kbar). The growth of garnet resumed after consumption of chlorite with substantial increase in pressure, and ceased as temperature increased to a maximum of 615 °C with a constant pressure of 6.5 Kbars (Lang, 1996). After the addition of kyanite to the assemblage, another rim garnet growth occurred with temperature decrease and pressure increase (Lang, 1996). By combining the reconstructed porphyroblast growth sequence with their FIA succession data, the staurolite FIA sets: A, B, C, D, E and F can be correlated to garnet FIA sets: II, III, IV, V, and VI respectively. A total of 6 FIA successions peaking at $47° \pm 13°$, $0° \pm 7°$, $89° \pm 12°$, $143° \pm 8°$, $8° \pm 22°$ and $83° \pm 5°$ was determined.

7. Foliation asymmetry within porphyroblasts across the domes

In order to determine the changes of kinematic conditions and the relative timing of folding events, the geometries of porphyroblast inclusion trails for each FIA sets were examined. The asymmetries of inclusion trail geometries were established by looking in a northerly direction on thin sections orthogonal of each FIA set. For E-W FIA sets, the asymmetries were established by looking on N-S-trending vertical thin sections toward west. Four types of asymmetries are separated, and they are: clockwise flat to steep foliations, anticlockwise flat to steep foliations, clockwise steep to flat foliations, and anticlockwise steep to flat foliations (Fig. 6a). The clockwise asymmetry refers to foliations with dextral curvature, while the anticlockwise asymmetry refers to sinistral curvature. The flat to steep group is defined by inclusion trails with a subhorizontal foliation curving into subvertical tails, and vice versa for the subvertical group.

Fig. 6b,c show histogram plots of the asymmetry of curvature of inclusion trails of garnet and staurolite porphyroblasts separated according to FIA sets and fold limbs. Exclusive anticlockwise asymmetry is recorded for steep to flat foliations from garnet FIA sets I and VI on both limbs, and set III on the west limb (Fig. 6c); staurolite FIA set A on the east limb and set C on the west limb (Fig. 6b). Nearly equal distribution between clockwise and anticlockwise asymmetries are recorded for steep to flat foliations from garnet FIA set II, IV and V, and staurolite FIA D on both limbs (Fig. 6b,c). Exclusive clockwise asymmetry is recorded for steep to flat foliation producing events from staurolite FIA set B on the east limb (Fig. 6b).

Nearly equal distribution between clockwise and anticlockwise asymmetries are recorded for flat to steep foliations from garnet FIA set I to IV on both limbs (Fig. 6c). Exclusive anticlockwise asymmetry is recorded for flat to steep foliations from garnet FIA set VI on west limbs, and staurolite set B on the east limb (Fig. 6b,c). Exclusive clockwise asymmetry is recorded for flat to steep foliations from garnet FIA set V on both limbs, and staurolite set B and E on the west limb (Fig. 6b,c). No change of asymmetry across the limbs can be observed other than staurolite FIA set B (Fig. 6b), but the asymmetry recorded by flat to steep foliations is opposite to expected as shown in Fig. 6a.

8. Interpretation

8.1. Timing of folds

Ramsay (1962a,b,c), and Powell and McQueen (1976) suggested there is a systematic relation between fold geometry and inclusion trail asymmetry preserved within syn-deformational porphyroblasts in areas where a fabric was initially orthogonal to the developing axial planar cleavage. This involves the inclusion trail asymmetry reversing across the axial trace of a fold

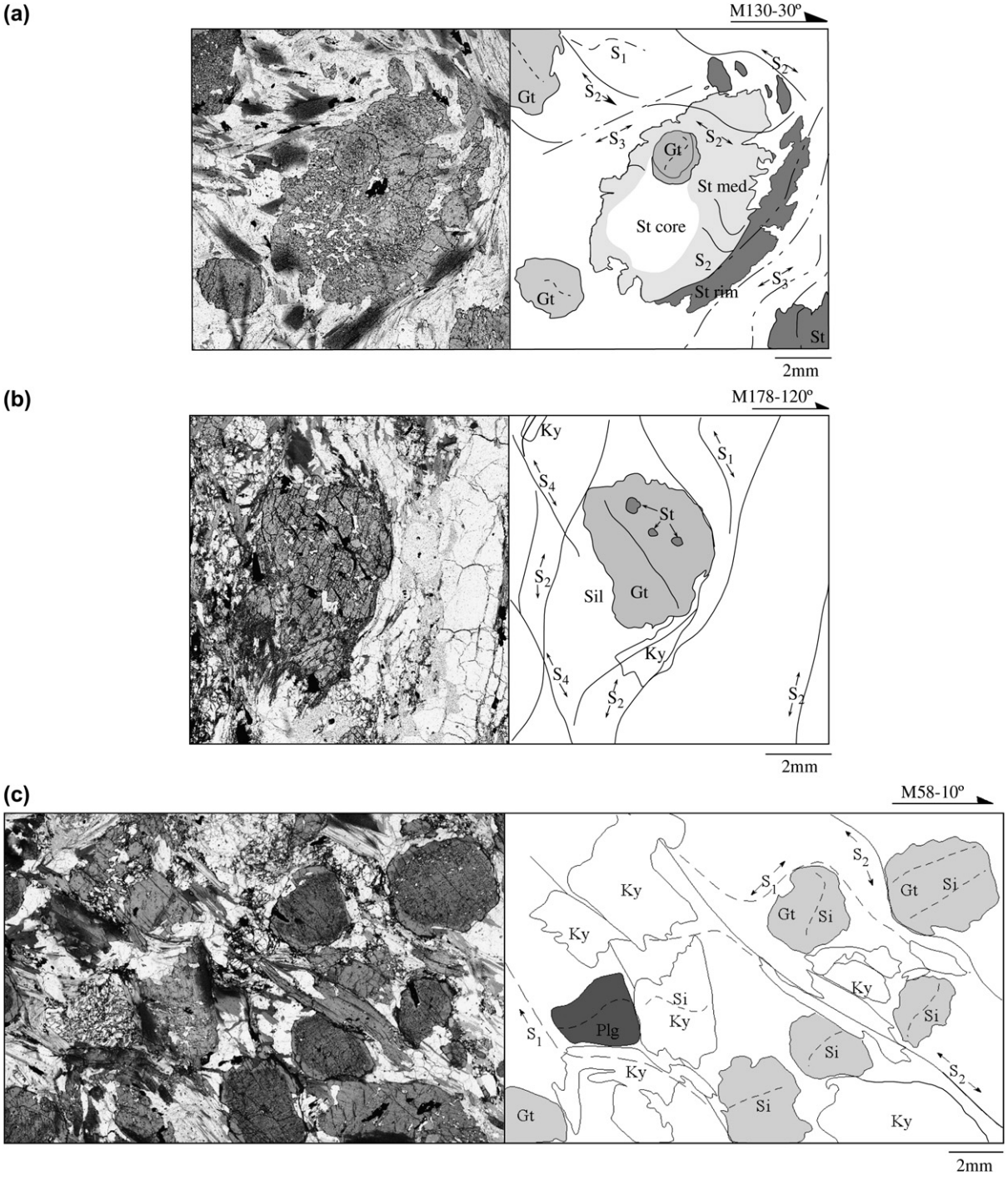

Fig. 5. Microphotographs and accompanying line diagrams showing the textural relation between staurolite (St), garnet (Gt), and kyanite (Ky) porphyroblasts and the matrix foliations. Vertical thin section, arrow indicates strike, plane polarized light. (a) Staurolite porphyroblasts contain garnet porphyroblast as inclusions and up to three period of growth can be distinguished, which are marked by various shades of grey. No trails can be distinguished in staurolite core region. Inclusion trails of mediam region are continuous with S_2 matrix foliation, truncated by the inclusion trails continuous with S_3 matrix foliation at the rim region. (b) Garnet porphyroblast with staurolite inclusions, inclusion trails parallel to S_1 but are truncated by the S_2 matrix foliation. Kyanite and fibrolitic sillimanite growth occur around the garnet rim. (c) Garnet porphyroblasts contain inclusion free rims and are in contact with kyanite porphyroblasts suggesting earlier growth of garnet compared to kyanite. Kyanite contains S_1 parallel inclusion trails truncated by the S_2 matrix foliation suggesting syn- or post-S_1 growth.

(Figs. 6a and 7a). In the case of the Baltimore gneiss domes, no such reverse of asymmetry was measured other than staurolite FIA set B (Fig. 6b,c). Because FIA set B trends almost perpendicular to the dome axis, the asymmetries recorded bear no relevance for determinations on the timing of the domes. Other than staurolite FIA set B, all east-west trending FIA data (garnet set II and VI, and staurolite set E) are omitted since they bear no relevance to the domes. Though no reverse of asymmetry was measured, this does not mean no folding had occurred. Bell et al. (2003, 2004) had demonstrated that it's quite

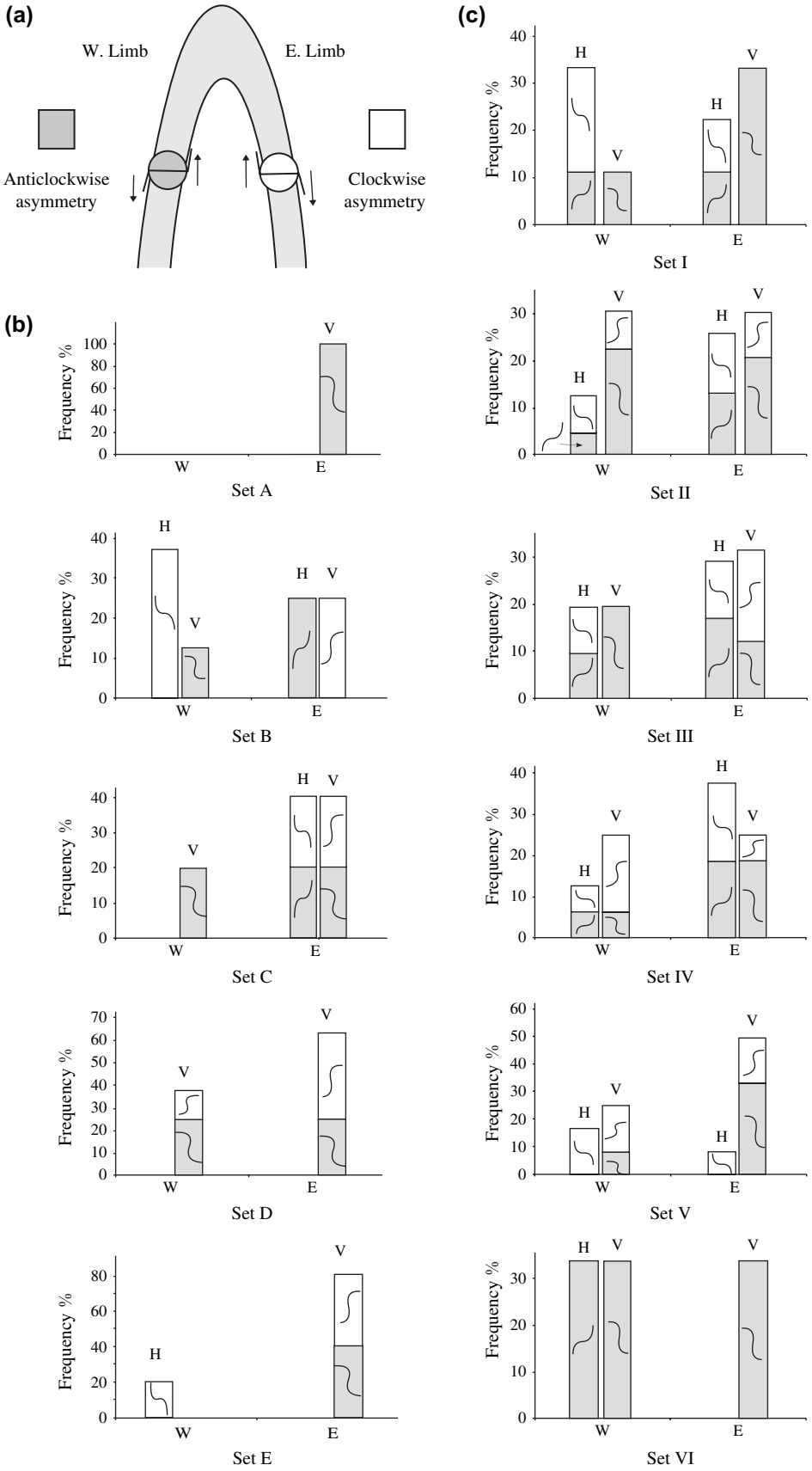

Fig. 6. Series of histograms of each FIA sets showing the asymmetry of inclusion trails preserved within porphyroblasts. Four asymmetry types: anticlockwise/clockwise flat to steep, and anticlockwise/clockwise steep to flat inclusion trail asymmetries are separated across fold limbs. (a) Expected asymmetry switch distribution across an anticline for syn-folding porphyroblasts − clockwise on the east limb, anticlockwise on the west limb. (b) and (c) show the percentage distribution of anticlockwise (gray columns) and clockwise (white columns) inclusion trails formed by vertical collapsing (V) and horizontal shortening (H) events recorded within (b) staurolite and (c) garnet porphyroblasts for each FIA sets across east (E) and west (W) limbs of the Baltimore gneiss anticlines.

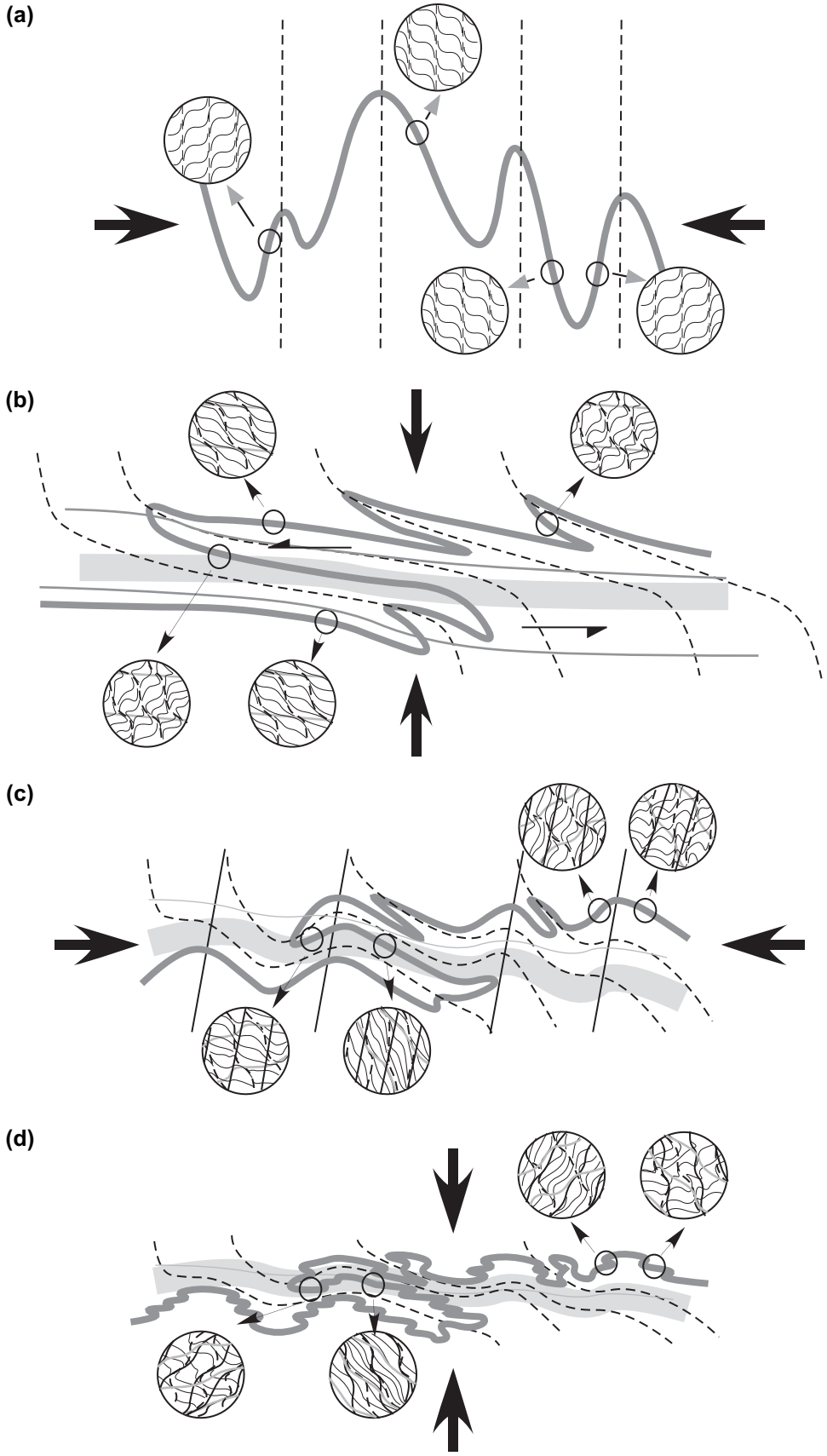

Fig. 7. Vertical schematic cross-section showing how gneiss domes formed by a refolded nappe with both clockwise and anticlockwise asymmetry for differentiated crenulation cleavages on both limbs. (a) Up-right regional folds formed by horizontal compression with expected opposite asymmetry across fold limbs. (b) With sinistral shear accompanied with gravitational collapsing, exclusive anticlockwise (top to left) asymmetry for steep to flat differentiated crenulation foliations formed along with the nappe. Both clockwise and anticlockwise asymmetry for flat to steep differentiated crenulation foliations are formed on both limbs. (c) and (d) Cycles of horizontal compression and vertical collapsing further reduced the fold amplitude of the nappe forming gneiss domes with both differentiated asymmetry forming on both limbs.

common to have both asymmetry trails for many FIA sets on both fold limbs, and suggested that this is the result of coaxial deformation at the bulk scale recorded by multiple periods of porphyroblast growth. They also argued that since no asymmetry switches that match those expected to accompany fold development can be found, the folding event should predate all porphyroblast growth. If this is also the case for the Baltimore gneiss domes, then these structures formed prior to Set I FIAs. As illustrated in Fig. 7a–c, if gneiss domes are produced by refolding, both differentiation asymmetries should be expected on both fold limbs (Fig. 7c). Though the pervasive matrix foliations, post-dates most porphyroblast growth, its folding around the Baltimore gneiss domes seems to indicate a late timing of the dome. However, this is contradicted by the foliation asymmetry and FIA data. Foliation reactivation and re-use are quite common for mutideformed terranes (Davis and Forde, 1994; Davis, 1995), with the original foliation being successively reactivated but rather then refolded, it would seems that the pervasive matrix foliations post-dates the fold.

8.2. Role of early nappe development

The asymmetries of inclusion trails preserved inside porphyroblasts, for each direction of bulk shortening, enable the dominant shear senses for each FIA set to be determined. As previous studies have suggested (Knopf and Jonas, 1929; Fisher et al., 1979; Muller and Chapin, 1984, Table 1), the Baltimore gneiss anticlines are part of a nappe system that has experienced multiple events of folding. If the gneiss domes were formed by diapiric rise of migmatitic gneisses, only clockwise flat to steep asymmetry should be recorded for the east limb while only anticlockwise flat to steep asymmetry should be recorded for the west limb. No such asymmetry pattern was recorded. The NE-SW trending set I FIA appears to be parallel to the general trend of macroscopic fold axes. Exclusive anticlockwise (top to the WNW) steep to flat inclusion trail asymmetry, formed during a gravitational collapse stage, was recorded for set I FIA samples (Figs. 6c and 7b). This indicates that this region had experienced strong northwestward shearing along a subhorizontal shearing plane during this time, which coincides with the west-verging nappe (Fig. 7b). Based on the exclusive anticlockwise asymmetry recorded by the oldest FIA set, the presence of an early nappe can be confirmed.

8.3. Deformation history of the Baltimore Gneiss Domes

Many metamorphic cores of orogenic belts exhibit large macroscopic folds outlined by a pervasive matrix foliations. This suggests the folds formed relatively late in the tectonic history, after development of that foliation. However, Adshead-Bell and Bell (1999) demonstrated, in the Adelaide fold belt of Australia, that map-scale folds are commonly formed early and subsequently suffer reorientations and attenuations during successive stages of bulk crustal shortening in different directions, but no major refolding. As Davis and Forde (1994) and Davis (1995) demonstrated, foliations in folded regions are commonly and repeatedly reactivated or re-used without being destroyed. Thus, it is reasonable for folds to have younger fabrics (due to successive reactivations) than the original folds. As stated before, the coaxial distribution of inclusion trail asymmetries across a fold was interpreted to post-date the fold. The presence of coaxial distribution of flat to steep foliation of the garnet FIA set I hints to the presence of an early formed NE-SW-trending up-right fold. However, without more definitive evidence, the formation of a west-verging nappe is tentatively interpreted as the first deformation event, pre-syn FIA set I (Fig. 8).

The coaxial nature of the inclusion trail asymmetries for the horizontal shortening portion of N-S trending FIA set II suggests that the first refolding occurred during this time (Figs. 7c and 8). FIA sets IV and C also showed coaxial asymmetries for flat to steep foliations (Fig. 7), suggesting that the refolded folds are progressively tightened by bulk horizontal shortening. With the oldest staurolite FIAs (set A) formed during the same time as the garnet FIA set III, this indicates that the peak metamorphism of the Taconian orogeny had occurred after the first refolding of the nappe event (D_1; Fig. 8). A similar repetition of coaxial tightening and flattening patterns has been noted in the Appalachians by Higgins (1973). As mentioned before, the presence of refolded isoclinal folds with sub-vertical axial planes in rocks of the Glenarm group is well documented throughout the Maryland Piedmont (Freedman et al., 1964; Fisher, 1970; Higgins, 1973; Muller and Chapin, 1984). Muller and Chapin (1984) interpreted that refolding of nappe commenced post the thermal peak of metamorphism during the Taconian orogeny because the metamorphic segregation layering within the Baltimore gneiss migmatites was folded. This was supported by Hall (1988) and Lang (1990) who found systematic variations in the estimated pressure at the peak of metamorphism during the Taconian orogeny along a NW-SE structural cross-section of the Baltimore region. However, the FIA and asymmetry results suggested much earlier refolding of the nappe. The refolded metamorphic isoclines noted by Muller and Chapin (1984), Hall (1988) and Lang (1990) reflect the later fold tightening event indicated by younger FIA set IV (Fig. 8). The young N-S trending garnet FIA set V recorded exclusive dextral sense of shear during horizontal compression (Fig. 7). The presence of dextral shear along the E-W fault resulted from the E-W collision between Avalon and Laurasia during the Taconian orogeny had been proposed (Thomas, 1977; Fisher et al., 1979; Thomas, 1983). Yeh and Bell (2004) further suggested this dextral reactivation had deformed the original NE-SW-trending central Appalachian mountain chain dextrally to its current position. Instead of coaxial bulk horizontal shortening, dextral bulk horizontal shortening should be expected during this time, and is indeed recorded by inclusion trail geometries.

9. Discussion

9.1. Development model of the gneiss domes

The anticlinal structures exposing basement gneiss around the Baltimore region have been cited as classic examples of

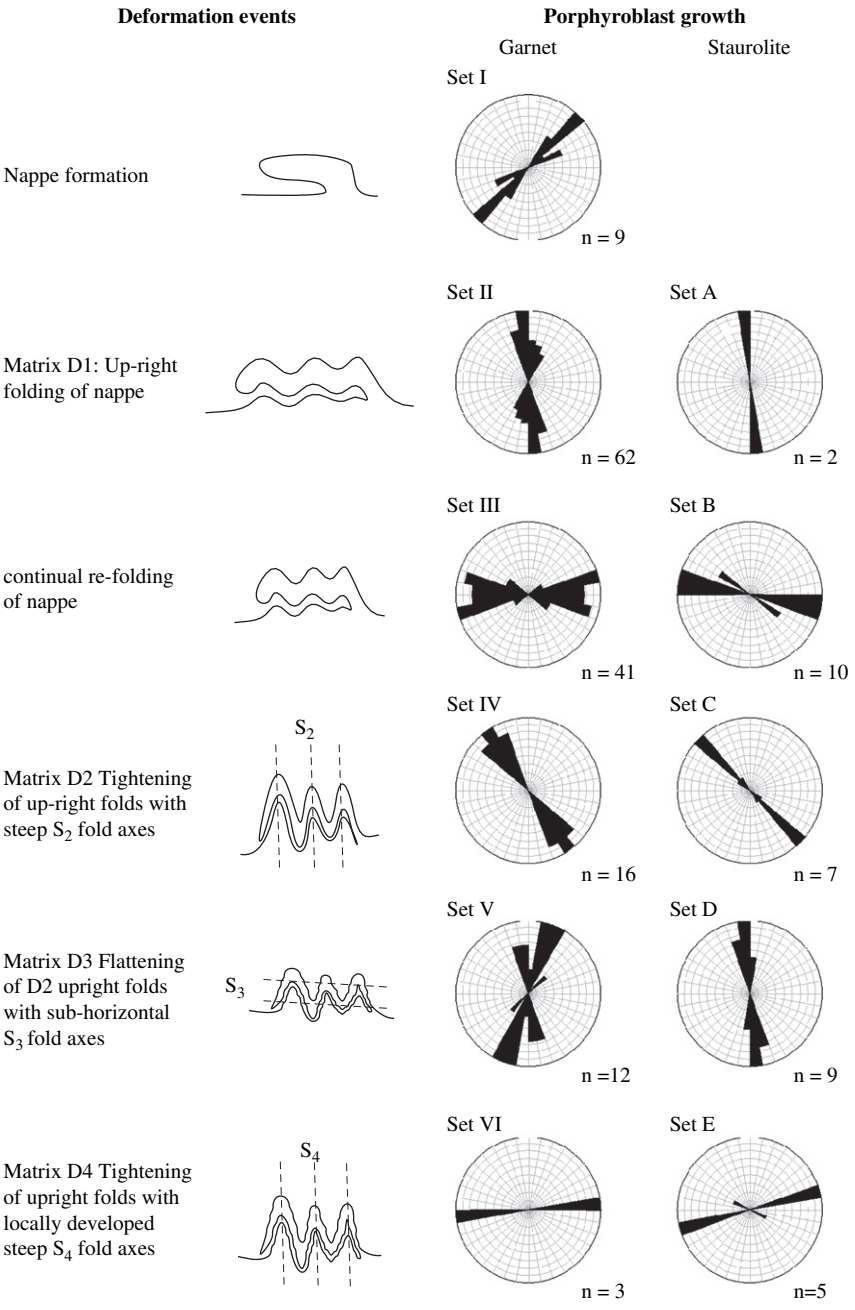

Fig. 8. Series of schematic diagrams showing the interpreted progressive development of the gneiss domes. The relative succession of FIA sets measured from garnet and staurolite porphyroblasts are shown with equal area (radii = square root of frequency) rose diagrams with a 10° class interval.

mantled gneiss domes formed by diapiric rise of migmatitic gneisses (Eskola, 1949). However, recent studies (Fisher, 1970; Muller and Chapin, 1984; Hall, 1988; Lang, 1990, 1991; Fisher and Olsen, 2004) including the present paper suggest that they are the result of interference between multiple upright folds that refolded early nappe structures. According to previous studies (Fisher, 1970; Muller and Chapin, 1984; Hall, 1988; Lang, 1990, 1991), the nappe formed at an early stage of the deformation sequences, and experienced multiple refolding events during the Taconic and Acadian orogenies. Evidence of microfabric asymmetry for nappe development during the gravitational collapse portions of FIA set I coincide with an early timing of nappe development as interpreted by Higgins (1973), and Muller and Chapin (1984).

As Bell et al. (2003, 2005) had shown, the overall coaxial deformation is a common feature around gneiss domes since granitoids are generally considered as relatively homogenous masses. Due to this character, deformation tends to partition around them, thus making the granitoids form the cores of folds, and preventing them from being further deformed by younger deformations. Such a coaxial nature of deformation is also recorded by inclusion trails within porphyroblasts. Detailed microstructural measurements conducted in this study better supports the nappe-and-dome model (e.g., Hopson, 1964;

Higgins, 1973; Fisher et al., 1979; Muller and Chapin, 1984) than the diaprism model (Eskola, 1949; Teyssier and Whitney, 2002).

9.2. The implications of inclusion trail asymmetries and FIA orientations for macro-scale deformation

The succession of 6 FIA trends preserved in garnet and staurolite porphyroblasts around the domes in the vicinity of Baltimore region can not be explained by porphyroblast rotation. If the porphyroblasts had rotated as the inclusion trails were overgrown, enormous spreads and randomized FIA trends and successions should be expected. However, statistical results (Table 3) indicate the FIA populations are not random, and the succession is consistent (Table 2). Furthermore, the inclusion trail asymmetries should be exactly opposite to those that observed if a NW-moving nappe had developed in the manner suggested by Rosenfeld (1968) for southeast Vermont, USA. The consistency of the FIA succession and orientations across the gneiss domes, and the anticlockwise inclusion trail asymmetries reveal that these porphyroblasts did not form by rotation during nappe development. Nor were they rotated by any younger deformations. Thus, timing of the folds and deformation history reconstruction by separating the differentiation asymmetry preserved within porphyroblasts according to FIA succession is applicable in this region.

Shear sense determinations along foliations in deformed and metamorphosed rocks are an important element of structural analysis, providing constraints on kinematic paths, and possibly metamorphic paths, during orogenesis. Since Zwart (1960), shear sense interpretations based on the inclusion-trail geometries were considered as a product of rotation of the porphyroblasts during growth, conflicting with the known displacement along movement zones (e.g., Bell and Johnson, 1992). The dominant asymmetries of inclusion trails preserved inside of porphyroblasts for each direction of bulk shortening indicated by the FIA (e.g., Bell et al., 1998) enable determination of the major shear senses that generated these microstructures. Bell and Johnson (1992) pointed out that, since deformation partitioning controls the development of new foliations in part by the rotation of older ones, the geometry developed must reflect the strain field. Therefore, to determine the local shear sense for a particular deformation event, one needs only to distinguish the curvature of earlier formed foliation into a later one (that is from zones of low strain to zones of high strain). The long and complex deformation histories recorded by inclusion trails inside porphyroblasts appear to allow the determination of local shear senses for generations of foliations that predate the matrix. This study also shows that FIA and inclusion trail asymmetries can be used to determine a detailed kinematic history plus a history of folding of a complex deformed region.

10. Conclusion

Detailed microstructural analysis indicates that the gneiss domes around the Baltimore region formed by folding an early nappe and not by diapiric rise of migmatitic gneisses. A succession of six FIA (Foliation Intersection Axes) sets, based upon relative timing of inclusion texture in garnet and staurolite porphyroblasts, revealed 6 superposed deformation phases. Establishing the timing of the development of macroscopic folds, that have undergone a long and complex deformation history, is potentially difficult. The exclusive top to west bottom to east asymmetry of the inclusion trails recorded by the oldest FIA set I, as examined on the limbs of these domes, and the same NE-SW trend between FIA set and the nappe indicate that the nappe formed with a western vergence with an early timing of the deformation sequence. Despite the fact that nappe formation and part of its refolding history predate the principal matrix foliations, these events can be reconstructed based on the preservation of the corresponding fabric generations in different sets of porphyroblasts with their original orientations.

Acknowledgements

The earlier version of the manuscript has benefited greatly from a through and constructive review by Domingo Aerden, Tim Bell, and Gary Solar that I wish to fully acknowledge. I also thank S.C. Fang and Ken Hickey for providing valuable suggestions on statistical analyses. The final English polishing from Charles Hutchison is greatly appreciated. This work was part of a PhD dissertation and was supported by the Earth Science Department, James Cook University, Australia.

References

Adshead-Bell, N.S., Bell, T.H., 1999. The progressive development of a macroscopic upright fold pair during five near-orthogonal foliation-producing events: complex microstructures versus a simple macrostructure. Tectonophysics 306, 121–147.

Aerden, D.G.M., 1994. Kinematics of orogenic collapse in the Variscan Pyrenees deduced from microstructures in porphyroblastic rocks from the Lys-Caillaouas massif. Tectonophysics 238, 139–160.

Aerden, D.G.M., 1998. Tectonic evolution of the Montagne Noire and a possible orogenic model for syn-collisional exhumation of deep rocks, Hercynian belt, France. Tectonics 17, 62–87.

Aleinikoff, J.N., Fanning, C.M., Horton, Jr., J.W., Drake, Jr., A.A., Sauer, R.R., 1997. The Baltimore Gneiss Re-revisited: New SHRIMP (zircon) and conventional (titanite) U-Pb ages [abstract]: GAC/MAC Annual Meeting, May 19–21, Abstract Volume, A-2.

Aleinikoff, J.H., Horton Jr., J.W., Drake Jr., A.A., Fanning, C.M., 2002. Shrimp and conventional U-Pb ages of Ordovician granites and tonalities in the central Appalachian piedmont: implications for Paleozoic tectonic events. American Journal of Science 302, 50–75.

Andersen, A., Hartz, E.H., Vold, J., 1998. A late orogenic extensional origin for the infracrustal gneiss domes of the East Greenland Caledonides (72–74°N). Tectonophysics 285, 353–369.

Bell, T.H., 1986. Foliation development and refraction in metamorphic rocks; reactivation of earlier foliations and de-crenulation due to shifting patterns of deformation partitioning. Journal of Metamorphic Geology 4/4, 421–444.

Bell, T.H., Hayward, N., 1991. Episodic metamorphic reactions during orogenesis: the control of deformation partitioning on reaction sites and duration. Journal of Metamorphic Geology 9, 619–640.

Bell, T.H., Johnson, S.E., 1989. Porphyroblast inclusion trails: the key to orogenesis. Journal of Metamorphic Geology 10, 99–124.

Bell, T.H., Johnson, S.E., 1992. Shear sense: a new approach that resolves conflicts between criteria in metamorphic rocks. Journal of Metamorphic Geology 10, 99–124.

Bell, T.H., Ford, A., Wang, J., 1995. A new indicator of movement direction during orogenesis: measurement technique and application to the Alps. Terra Nova 7, 500–508.

Bell, T.H., Hickey, K.A., Upton, J.G., 1998. Distinguishing and correlating multiple phases of metamorphism across a multiply deformed region using the axes of spiral, staircase and sigmoidal inclusion trails in garnet. Journal of Metamorphic Geology 16, 767–794.

Bell, T.H., Ham, A.P., Hickey, K.A., 2003. Early formed regional antiforms and synforms that fold younger matrix schistosities: their effect on sites of mineral growth. Tectonophysics 367, 253–278.

Bell, T.H., Ham, A.P., Kim, H.S., 2004. Partitioning of deformation along an orogen and its effects on porphyroblast growth during orogenesis. Journal of Structural Geology 26, 825–845.

Bell, T.H., Ham, A.P., Hayward, N., Hickey, K.A., 2005. On the development of gneiss domes. Australian Journal of Earth Science 52, 183–204.

Bosbyshell, H., Sinha, A.K., Crawford, M.L., Fleming, P., Srogi, L., Lutz, T.M., 1998. Thermal evolution of a convergent orogen; new U/Pb ages of monazite and zircon from the Central Appalachian Piedmont. Geological Society of America. Abstracts with Programs 30/7, 125.

Bosbyshell, H., Williams, M., Jercinovic, M., Crawford, M., 1999. Electron microprobe age mapping and dating of monazite; new insights on the timing of polyphase Paleozoic metamorphism in the Central Appalachians. Geological Society of America. Abstracts with Programs 31/7, 39.

Bromery, R.W., 1968. Geological Interpretation of Aeromagnetic and Gravity Surveys of the Northeastern End of the Baltimore—Washington Anticlinorium, Harford, Baltimore, and Part of Carroll County, Maryland [Ph.D. dissertation]. Johns Hopkins University, Baltimore, Maryland.

Burg, J.P., Guiraud, M., Chen, G.M., Li, G.C., 1984. Himalayan metamorphism and deformations in the north Himalayan Belt (southern Tibet, China). Earth and Planetary Science Letters 69, 391–400.

Cleaves, E.T., Edwards, J., Glaser, J., 1986. Geologic Map of Maryland. Maryland Geological Survey.

Cloos, E., 1964. Structural geology of Howard and Montgomery counties. In: The Geology of Howard and Montgomery Counties. U.S. Geological Survey, pp. 216–261.

Crowley, W.P., 1976. The Geology of the Crystalline Rocks Near Baltimore and Its Bearing on the Evolution of the Eastern Maryland Piedmont. Annapolis, MD. Maryland Geological Survey.

Crowley, W.P., 1977. Geologic Map of the Reisterstown Quadrangle, Maryland. 1:24,000. Reisterstown Quadrangle. Geology, Hydrology and Mineral Resources, Maryland, USA. State of Maryland Natural Resources Maryland Geological Survey, Map 1.

Crowley, W.P., Reinhardt, J., 1975. Geologic Map of the Cockeysville Quadrangle, Maryland Cockeysville Quadrangle, Geology, Hydrology and Mineral Resources. Maryland, USA. State of Maryland Department of Natural Resources Maryland Geological Survey, Map 1, scale 1:24,000.

Crowley, W.P., Reinhardt, J., 1980. Geological Map of the Ellicott City Quadrangle, Maryland. 1:24000. Maryland, USA. State of Maryland Department of Natural Resources Maryland Geological Survey.

Crowley, W.P., Reinhardt, J., Cleaves, E.T., 1975. Geologic Map of the Cockeysville Quadrangle, Maryland. Maryland Geological Survey, scale 1:24,000.

Crowley, W.P., Reinhardt, J., Cleaves, E.T., 1976a. Geologic Map of Baltimore County and City. Maryland Geological Survey, scale 1:62,500.

Crowley, W.P., Reinhardt, J., Cleaves, E.T., 1976b. Geologic Map of the White Marsh Quadrangle, Maryland, White Marsh Quadrangle. Geology, Hydrology and Mineral Resources. Maryland, USA: State of Maryland Department of Natural Resources Maryland Geological Survey, Map 1, scale 1:24,000.

Davis, B.K., 1995. Regional-scale foliation reactivation and re-use during formation of a macroscopic fold in the Robertson River Metamorphics, North Queensland, Australia. Tectonophysics 242, 293–311.

Davis, B.K., Forde, A., 1994. Regional slaty cleavage formation and fold axis rotation by re-use and reactivation of pre-existing foliations: the Fiery Creek Slate Belt, North Queensland. Tectonophysics 230, 161–179.

Doe, B.R., Tilton, G.R., Hopson, C.A., 1965. Lead isotopes in feldspars from selected granitic rocks associated with regional metamorphism. Journal of Geophysical Research 70, 1947–1968.

Dorais, M.J., Wintsch, R.P., Becker, H., Kunk, M.J., 2001. The Massabesic Gneiss complex, New Hampshire: a study of a portion of the Avalon terrane. American Journal of Science 301, 657–682.

Drake Jr., A.A., 1989. Metamorphic rocks of the Potomac terrane in the Potomac Valley of Virginia and Maryland. In: International Geological Congress, 28, Field Trip Guidebook T202. American. Geophysical Union, 22, Washington, D.C.

Drake Jr., A.A., Sinha, A.K., Laird, J., Guy, R.E., 1989. The Taconic orogen. In: Hatcher Jr., R.D., Thomas, W.A., Viele, G.W. (Eds.), The Appalachian-uachita Orogen in the United States. The Geology of North America F-2. Geological Society of America, Boulder, Colorado, pp. 101–177.

Duckan, I.J., 1984. Structural evolution of the Thor – Odin gneiss dome. Tectonophysics 101, 87–130.

Eskola, P., 1949. The problem of mantled gneiss domes. Quarterly Journal of Geological Society of London 104/416, 461–476.

Fisher, G.W., 1970. The Metamorphose sedimentary rocks along the Potomac River near Washington, D.C. In: Fisher, G.W., Pettijohn, F.J., Reed, J.C. (Eds.), Studies of Appalachian Geology. John Wiley & Sons, Inc, USA, pp. 299–316.

Fisher, G.W., 1971. Kyanite-, Staurolite- and Garnet- Bearing Schists in the Setters Formation, Maryland Piedmont. Geological Society of America Bulletin 82, 229–232.

Fisher, G.W., Olsen, S.N., 2004. The Baltimore gneiss domes of the Maryland Piedmont. In: Whitney, D.L., Teyssier, C., Siddoway, C.S. (Eds.), Gneiss Domes in Orogeny. Geological Society of America Special Paper, 380, pp. 307–320.

Fisher, G., Higgins, M.Z., Zeitz, I., 1979. Geological interpretations of aeromagnetic maps of the Crystalline rocks in the Appalachians, Northern Virginia to New Jersey. Maryland Geological Survey Report of Investigations 32, 40.

Freedman, J., Wise, D.U., Bentley, R.D., 1964. Pattern of folded folds in the Appalachian Piedmont along Susquehanna River. Geological Society of America Bulletin 75, 621–638.

Grauert, B., 1973a. U-Pb isotopic studies of zircons from the Baltimore gneiss of the Townson Dome, Maryland. Carnegie Institution of Washington Year Book 72, 285–288.

Grauert, B., 1973b. U-Pb isotopic studies of zircons from the Gunpowder granite. Baltimore County. Maryland. Carnegie Institution of Washington Year Book 72, 285–288.

Hall, P.S., 1988. Deformation and Metamorphism of the Aluminous Schist Member of the Setters Formation, Cockeysville, Maryland [MsC dissertation]: West Virginia, West Virginia University.

Ham, A.P., Bell, T.H., 2004. Recycling of foliations during folding. Journal of Structural Geology 26, 1989–2009.

Hayward, N., 1990. Determination of early fold axis orientations in multiply deformed rocks using porphyroblast inclusion trails. Tectonophysics 179, 353–369.

Hickey, K., Bell, T.H., 2001. Timing fold development in multideformed terrains: the role of orthogonally overprinting foliations. Bulletin of the Geological Society of America 113, 1282–1298.

Higgins, M.W., 1972. Age, Origin, regional relations, and nomenclature of the Flenarm Series, central Appalachian Piedmont: A reinterpretation. Geological Society of America Bulletin, vol. 83, pp. 989–1026.

Higgins, M.W., 1973. Superimposition of folding in the Northeastern Maryland Piedmont and its bearing on the history and tectonics of the central Appalachians. American Journal of Science 273 (A), 150–195.

Hobbs, B.E., Means, W.D., Williams, P.F., 1976. An Outline of Structural Geology. Wiley & Sons, New York. 409–416.

Hopson, C.A., 1964. The Crystalline Rocks of Howard and Montgomery Counties. In: The Geology of Howard and Montgomery Counties. Maryland Geological Survey, pp. 27–215.

Johnson, S.E., 1992. Sequential porphyroblast growth during progressive deformation and low-p, high-t (lpht) metamorphism. Cooma Complex, Australia: the use of microstructural analysis in better understanding deformation and metamorphic histories. Tectonophysics 269, 311–340.

King, M., 1994. Fisheries Biology, Assessment and Management. Oxford, England, 301–306 p.

Knopf, E.B., Jonas, A., 1929. The geology of the crystalline rocks of Baltimore County. Maryland Geological Survey, Baltimore County. 97–199.

Kodama, K.P., Chapin, D.A., 1984. A detailed gravity study of the Chattolanee Baltimore Gneiss Dome, Maryland, U.S.A. Geophysical Research Letters 68, 286–296.

Lang, H.M., 1990. Regional variation in metamorphic conditions recorded by pelitic schists in the Baltimore Area, Maryland. Southeastern Geology 31/1, 27–43.

Lang, H.M., 1991. Quantitative Interpretation of within-outcrop variation in metamorphic assemblage in staurolite-kyanite-grade metapelites, Baltimore. Maryland. Canadian Mineralogist 29, 655–671.

Lang, H.M., 1996. Pressure-temperature-reaction history of metapelitic rocks from the Maryland Piedmont on the basis of correlated garnet zoning and plagioclase-inclusion composition. American Mineralogist 81, 1460–1475.

Lee, J., Hacker, B., Wang, Y., 2004. Evolution of North Himalayan gneiss domes: structural and metamorphic studies in Mabja Dome, southern Tibet. Journal of Structural Geology 26, 2297–2316.

Moller, S.A., 1979. Geologic Map of the Phoenix Quadrangle, Maryland. 1:24,000. Maryland, USA. State of Maryland Department of Natural Resources Maryland Geological Survey.

Muller, P.D., 1991. Geologic Map of the Hampstead Quadrangle, Maryland, USA. State of Maryland Department of Natural Resources Maryland Geological Survey, scale 1:24,000.

Muller, P.D., Chapin, D.A., 1984. Tectonic evolution of the Baltimore gneiss anticlines, Maryland. Geological Society of America Special Paper 194, 127–148.

Muller, P.D., Edwards, J., 1985. Tectonostratigraphic relationships in the central Maryland Piedmont. The Geological Society of America, Northeastern Section, 20th annual meeting: Abstracts with Programs 17/1, 55.

Olsen, S.N., 1999. Petrology of the Baltimore Gneiss in the northeast Towson Dome, Maryland Piedmont. In: Valentino, D.W., Gates, A.E. (Eds.), The Mid-Atlantic Piedmont: Tectonic Missing Link of the Appalachians. Geological Society of America Special Paper, 330, pp. 111–124.

Pavlides, L., 1989. Early Paleozoic composite mélange terrane, central Appalachian Piedmont, Virginia and Maryland: its origin and tectonic history. In: Horton Jr., J.W., Rast, N. (Eds.), Mélanges and Olistostromes of the United States Appalachians. Geological Society of America Special Paper, pp. 135–193.

Plank, M.O., 1989. Metamorphism in the Wissahickon Formation of Delaware and adjacent areas of Maryland and Pennsylvania [MsC dissertation]. Newark, University of Delaware.

Powell, D., MacQueen, J.A., 1976. Relationships between garnet shape, rotational inclusion fabrics and strain in some Moine metamorphic rocks of Skye, Scotland. Tectonophysics 35/4, 391–402.

Powell, C., Vernon, R.H., 1979. Growth and rotation history of garnet porphyroblasts with inclusion spirals in a Karakoram Schist. Tectonophysics 54, 25–43.

Ramsay, J.G., 1962a. Interference patterns produced by the superposition of folds of "similar type". Journal of Geology 70/4, 466–481.

Ramsay, J.G., 1962b. The geometry and mechanics of formation of "similar type" folds. Journal of Geology 70/3, 309–327.

Ramsay, J.G., 1962c. The geometry of conjugate fold systems. Geological Magazine 99/6, 516–526.

Ratcliffe, N.M., Armstrong, T.R., Tracy, R.J., 1992. Tectonic-cover basement relations and metamorphic conditions of formation of the Sadawga, Rayponda and Athens domes, southern Vermont. Guidebook for field trips in the Connecticut Valley region of Massachusetts and adjacent states, Geology Department, University of Massachusetts 66, 257–290.

Rosenfeld, J.L., 1968. Garnet rotations due to the major Paleozoic deformations in Southeast Vermont. In: Zan, E., White, W.S., Hadley, J.B., Thompson, J.B. (Eds.), Studies of Appalachian Geology. John Wiley & Sons, Inc, USA, pp. 185–202.

Rosenfeld, J.L., Christensen, J.N., DePaolo, D.J., 1988. Snowball garnets revisited, southeastern Vermont. New England intercollegiate geological conference 80th annual meeting, Guidebook for field trips in southwestern New Hampshire, southeastern Vermont, and north-central Massachusetts. Geological Society, 223–240.

Seiders, V.M., Higgins, M.W., 1976. Age, origin, regional relations and nomenclature of the Glenarm Series, central Appalachian Piedmont: a reinterpretation: discussion and replay. Geological Society of America Bulletin 87, 1519–1528.

Sinha, A.K., Hanan, B.B., 1987. Age, origin, and tectonic affinity of the Baltimore Mafic Complex. Geological Society of America, Maryland. Abstract with Programs 19/2, 129.

Sinha, A.K., Hanan, B., Wayne, D.M., 1997. Igneous and metamorphic U-Pb zircon ages from the Baltimore mafic complex, Maryland Piedmont. Geological Society Memoir 191, 275–286.

Smith, J.V., Marshall, B., 1992. Patterns of folding and fold interference in oblique contraction of layered rocks of the inverted Cobar Basin, Australia. Tectonophysics 215, 319–334.

Southwick, D.L., Fisher, G.W., 1967. Revision of stratigraphic nomenclature of the Glenarm Series in Maryland. Maryland Geological survey Report of Investigations 6, 19.

Southwick, D.L., Owens, J.P., 1968. Geologic map of Harford County. Maryland Geological Survey, USA.

Teyssier, C., Whitney, D.L., 2002. Gneiss domes and orogeny. Geology 30, 1139–1142.

Thomas, W.A., 1977. Evolution of Appalachian-Ouachita salients and recesses from reentrants and promontories in the continental margin. American Journal of Science 277, 1233–1278.

Thomas, W.A., 1983. Continental margins, orogenic belts, and intracratonic structures. Geology 11, 270–272.

Tilton, G.R., Doe, B.R., Hopson, C.A., 1970. Zircon age measurements in the Maryland Piedmont, with special reference to Baltimore Gneiss Problems. In: Fisher, G.W., Pettijohn, F.J., Reed, J.C. (Eds.), Studies of Appalachian Geology- Central and Southern. John Wiley & Sons, Inc, USA, pp. 429–434.

Upton, G.J., Fingleton, B., 1989. Spatial Data Analysis by Example. Wiley & Sons, New York, p. 2.

Vernon, R.H., 1988. Microstructural evidence of rotation and non-rotation of mica porphyroblasts. Journal of Metamorphic Geology 6, 595–601.

Viruete, J.E., 1998. Relationships between structural units in the Tormes gneiss (NW Iberian massif, Spain): geometry, structure and kinematics of contractional and extensional Variscan deformation. Geologische Rundschau 87, 165–179.

Wetherill, G.W., Tilton, G.R., Davis, G.L., Hart, S.R., Hopson, C.A., 1966. Age measurements in the Maryland Piedmont. Journal of Geophysical Research 71/8, 2139–2155.

Williams, H., 1978. Tectonic Lithofacies Map of the Appalachian Orogen, Map No. 1. Memorial University of Newfoundland.

Williams, P.F., 1985. Multiply deformed terrains-problems of correlation. Journal of Structural Geology 7 (3/4), 269–280.

Wise, D.U., 1970. Multiple deformation, geosynclinal transitions and the matrix problem in Pennsylvania. In: Fisher, G.W., Pettijohn, F.J., Reed, J.C. (Eds.), Studies of Appalachian Geology- Central and Southern. John Wiley & Sons, Inc, USA, pp. 317–334.

Yeh, M.W., 2003. The significance and application of Foliation Intersection/Inflection Axes (FIA) within porphyroblasts: a review. Terrestrial, Atmospheric and Oceanic Sciences 14/4, 401–419.

Yeh, M.W., Bell, T.H., 2004. Significance of dextral reactivation of an E-W transfer fault in the formation of the Pennsylvania orocline, central Appalachians. Tectonics 23, TC5009.

Zwart, H.J., 1960. The chronological succession of folding and metamorphism in the Central Pyrenees. Geologische Rundschau 50, 203–218.